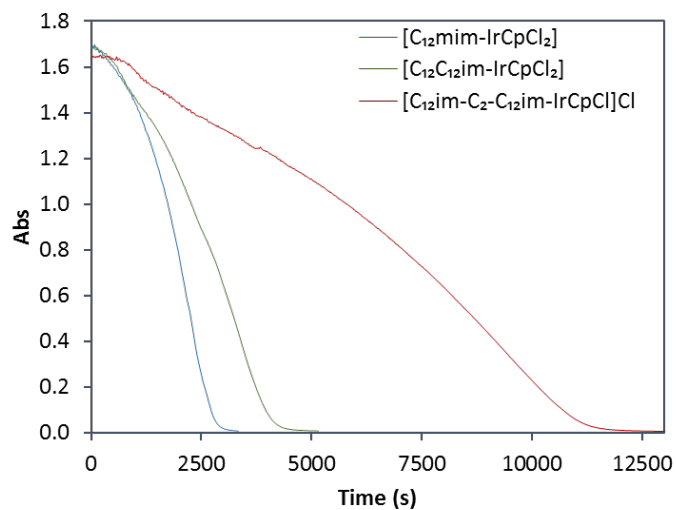
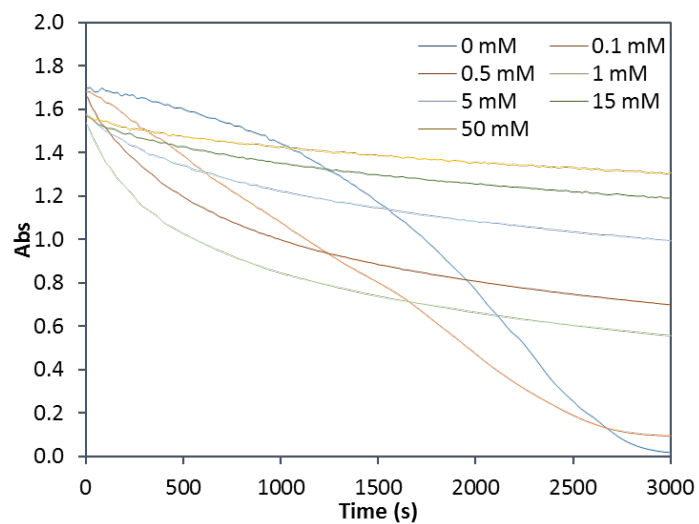




## 1 Reaction profiles



**Figure S1** Representative kinetic profiles for the three new catalysts at concentration of 2  $\mu$ M and CAN 3 mM in HNO<sub>3</sub> 0.1 M



**Figure S2** Reaction profiles for catalyst 2  $\mu$ M and CAN 3 mM with different concentrations of additional [C<sub>12</sub>mim]Cl in HNO<sub>3</sub> 0.1 M

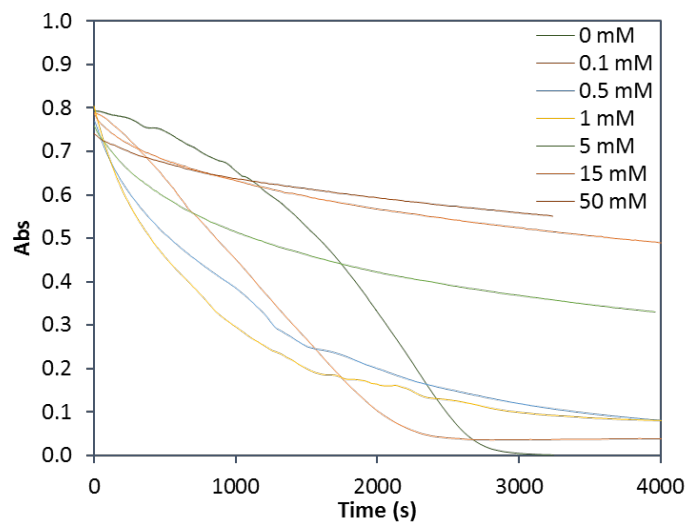


**Figure S3** Reaction profiles for catalyst **2**  $2\mu\text{M}$  and CAN  $1.5\text{ mM}$  with different concentrations of additional  $[\text{C}_{12}\text{mim}]\text{Cl}$  in  $\text{HNO}_3$   $0.1\text{ M}$

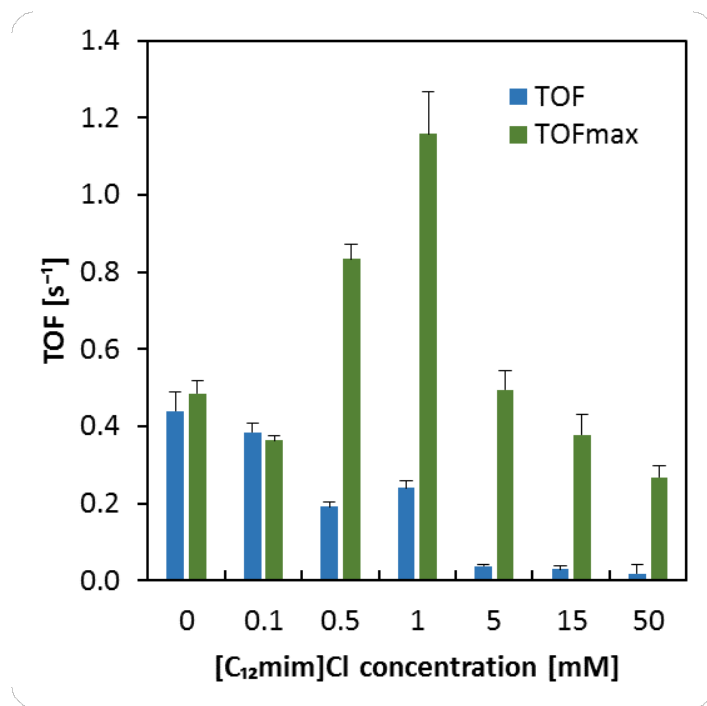


**Figure S4**  $TOF_{(t)}$  and  $TOF_{\text{max}}$  for catalyst **2**  $2\mu\text{M}$  and CAN  $1.5\text{ mM}$  with different concentrations of additional  $[\text{C}_{12}\text{mim}]\text{Cl}$  in  $\text{HNO}_3$   $0.1\text{ M}$

## 2 Reaction kinetics

We assume that the depletion of the  $Ce^{4+}$  can be described by

$$[Ce^{4+}](t) = a_1 e^{-k_1 t} + \frac{a_2}{(1-b_2) + b_2 e^{k_2 t}} \quad (S1)$$

with the initial absorbance  $a_0 = a_1 + a_2$ . The first part on the right hand side is a first order reaction. The second part stems from an autocatalyzed reaction.  $a_1$  and  $a_2$  are the relative importance of the two processes. If, for example,  $a_1$  is almost  $a_0$ , then the overall reaction follows first order, if  $a_2$  is almost  $a_0$  the reaction is determined by the autocatalyzed process.  $k_1$  and  $k_2$  are the corresponding rate constants in Hz. The parameter  $b_2$  describes the position of the turn point of the logistic function.

Eq. (S1) can be reformulated

$$a_1 e^{-k_1 t} + \frac{a_2}{(1-b_2) + b_2 e^{k_2 t}} = a_1 e^{-k_1 t} + \frac{\tilde{a}_2}{1 + e^{k_2(t-t_0)}} \quad (S2)$$

using  $\tilde{a}_2 = a_2/(1-b_2)$  and  $t_0 = \ln((1-b_2)/b_2)$ . Here,  $t_0$  corresponds to the time when half of the second process had taken place.

### 2.1 Rationalization

A first order reaction can be described by

$$-\frac{d[Ce^{4+}]}{dt} = k_1 [Ce^{4+}]. \quad (S3)$$

Solving this differential equation yields the first part of Eq. (S1).

In principle, the differential equation of the pure autocatalytic part looks like

$$-\frac{d[Ce^{4+}]}{dt} = k' [Ce^{4+}] + k'' [Ce^{4+}] \left( [Ce^{4+}]_0 - [Ce^{4+}] \right) \quad (S4)$$

resulting in

$$[Ce^{4+}](t) = \frac{[Ce^{4+}]_0 ([Ce^{4+}]_0 \cdot k'' + k')}{k' e^{([Ce^{4+}]_0 k'' + k')t} + [Ce^{4+}]_0 k'} \quad (S5)$$

Substituting  $k_2 = [Ce^{4+}]_0 k'' + k'$  and  $k' = k_2 \cdot b_2$  one yields

$$[Ce^{4+}](t) = \frac{[Ce^{4+}]_0}{1 - b_2 + b_2 e^{k_2 t}} \quad (S6)$$

which is similar to the logistic function of Eq. (S1).

### 2.2 Turn over frequency of the autocatalyzed reaction

The time-dependent concentration of the product,  $[Ce^{3+}](t)$ , should be  $[Ce^{4+}]_0 - [Ce^{4+}](t)$ . Consequently, the rate  $r(t)$  of  $Ce^{3+}$ -production is

$$r(t) = \frac{d[Ce^{3+}]}{dt} \simeq \frac{[Ce^{4+}]_0}{a_0} \cdot \frac{a_2 \cdot k_2 \cdot b_2 e^{k_2 t}}{(1-b_2 + b_2 e^{k_2 t})^2} \quad (S7)$$

neglecting the first order reaction. The maximum rate  $r$  is reached at

$$t_{max} = \frac{\ln(1-b_2) - \ln(b_2)}{k_2} \quad (S8)$$

As a result, the maximum turn-over-frequency

$$TOF = \frac{r(t_{max})}{[cat]} = \frac{a_2 \cdot k_2 \cdot [Ce^{4+}]_0}{4(1-b_2) \cdot a_0 \cdot [cat]} \quad (S9)$$

### 2.3 Turn over frequency of the first order reaction

In the rare case, that the depletion of  $[Ce^{4+}]$  follows a first order reaction without the autocatalyzed process, i.e.  $a_1 \simeq a_0$  and

$$r(t) = \frac{d[Ce^{3+}]}{dt} \simeq \frac{[Ce^{4+}]_0}{a_0} a_1 \cdot k_1 \cdot e^{-k_1 t}, \quad (S10)$$

the turn-over-frequency has its maximum value at  $t = 0$ :

$$TOF = \frac{[Ce^{4+}]_0 \cdot a_1 \cdot k_1}{[cat] \cdot a_0} \quad (S11)$$

The last value can also be gained from a Taylor-series expansion of the  $[Ce^{3+}](t)$

$$[Ce^{3+}] = [Ce^{4+}]_0 \left(1 - \frac{a_1}{a_0} e^{-k_1 t}\right) \quad (S12)$$

$$= [Ce^{4+}]_0 (1 - e^{-k_1 t}) \quad (S13)$$

$$\simeq [Ce^{4+}]_0 \left(1 - (1 - k_1 t + \dots)\right) \quad (S14)$$

$$\simeq [Ce^{4+}]_0 \cdot k_1 \cdot t \quad (S15)$$

since  $a_1 = a_0$  is the initial assumption of this rare case. The slope of Eq. (S15) is  $[Ce^{4+}]_0 \cdot k_1$  which has to be divided by  $[cat]$  to get the turn-over-frequency.

## 2.4 Mean reaction time

Since the maximum TOF might not be appropriate to characterize the efficiency of a catalyst in a chemical reaction as the time spent at the maximum TOF level does not enter the efficiency considerations. A lower maximum TOF level maintained over a longer period of time may result in a faster reaction overall.

As alternative property to characterize the promotion of the chemical reaction due to the catalyst or reaction conditions, one may look at the average reaction time

$$\langle t \rangle = \int_0^{\infty} \frac{[Ce^{4+}](t)}{[Ce^{4+}](0)} dt \quad (S16)$$

Here,  $[Ce^{4+}](t)$  is the time-dependant concentration of  $Ce^{4+}$  and  $[Ce^{4+}](0)$  its initial value. Integrating eq. (S1) yields

$$\langle t \rangle = \frac{1}{a_1 + a_2} \left[ a_2 \frac{\ln(b_2(e^{k_2 t} - 1) + 1) - k_2 t}{(b_2 - 1)k_2} - \frac{a_1 e^{-k_1 t}}{k_1} \right]_0^{\infty} \quad (S17)$$

For longer times  $t$  the first part of the right hand side can be simplified to  $a_2 \ln b_2 / ((b_2 - 1)k_2)$ . As result, eq. (S17) is

$$\langle t \rangle = \frac{\frac{a_2 \ln b_2}{(b_2 - 1)k_2} + \frac{a_1}{k_1}}{a_1 + a_2} \quad (S18)$$

The turn-over-frequency at the mean reaction time is

$$TOF(\langle t \rangle) = \frac{[Ce^{4+}]_0}{(a_1 + a_2)[cat]} \cdot \left( a_1 k_1 e^{-k_1 \langle t \rangle} + \frac{a_2 b_2 k_2 e^{k_2 \langle t \rangle}}{\left(1 - b_2 + b_2 e^{k_2 \langle t \rangle}\right)^2} \right) \quad (S19)$$

### 3 SAXS measurements

SAXS measurements were performed using a Bruker Nanostar (Bruker AXS) equipped with microfocus X-ray source (Incoatec ImS High Brilliance) with  $\text{CuK}\alpha$  radiation with a wavelength of 0.1542 nm, a pinhole camera and a 2D-position sensitive detector (Vantec 2000). The samples were filled into glass capillaries (1.5 mm diameter, 10  $\mu\text{m}$  wall thickness, from Hilgenberg). Scattering patterns were recorded for 6 hours, azimuthally integrated and corrected for background scattering from the capillary. The integrated intensity is shown in Fig. S5 in dependence on the scattering vector  $q = (4\pi/\lambda) \sin\Theta$ , with  $2\Theta$  being the scattering angle (black line). The red line is a fit with a core-shell model as in ref. 25 of the paper. Additionally, a power-law term was added to describe the strong intensity increase towards low  $q$ -values. The fit results in a core radius of 0.75 nm, a shell thickness of 2.1 nm and a value of 0.035 for the scaled medium contrast  $\gamma$ .

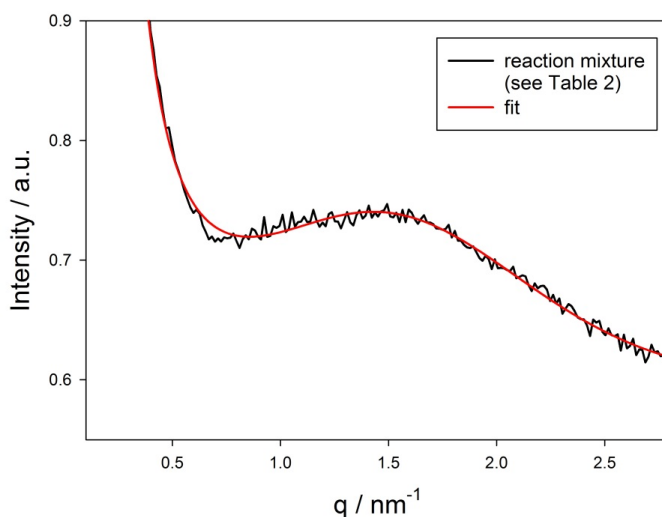


**Figure S5** SAXS intensity for the reaction mixture (as described in Table 2 of the paper), black line, together with fit from the core-shell model, red line

### 4 Ionic liquid stability

Stability experiments were done in 10 mL screw cap vials equipped with magnetic stirrer and thermostat at 25° C. 20  $\mu\text{l}$  of stock solution in acetonitrile of the catalyst 2 were added to 2 ml of  $\text{HNO}_3$  0.1 M Milli-Q water solution containing 50  $\mu\text{M}$  of  $\text{C}_{12}\text{mim-Cl}$ . Afterwards 1 ml of freshly prepared cerium ammonium nitrite stock solution in  $\text{HNO}_3$  0.1 M in Milli-Q water and 1 ml of  $\text{HNO}_3$  0.1 M in Milli-Q water were added to the vials, respectively. After one hour, the aqueous phases were extracted with dichloromethane 5 times. The combined organic phases were dried on  $\text{Na}_2\text{SO}_4$ , filtered, and evaporated in vacuo. The ionic liquid stability against oxidation was proven by comparing the  $^1\text{H}$  NMR spectra of the two reactions.

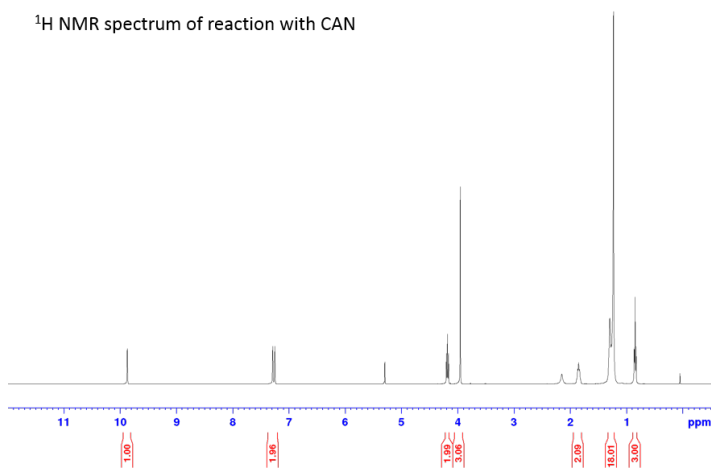
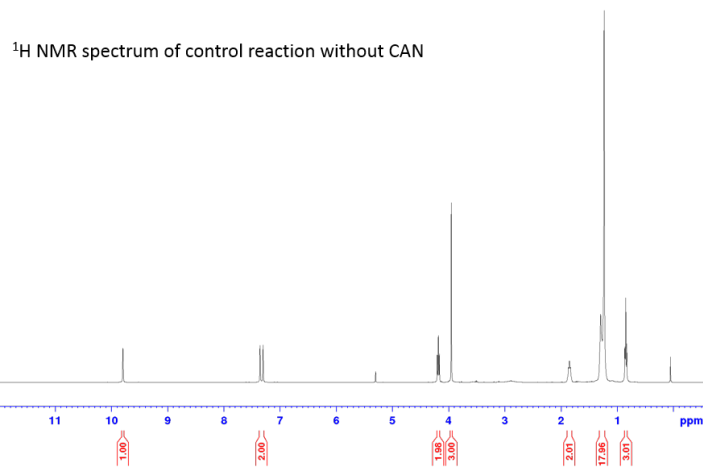


**Figure S6** Proof of ionic liquid stability under oxidative conditions